American Journal of
Computing and Engineering
(AJCE)

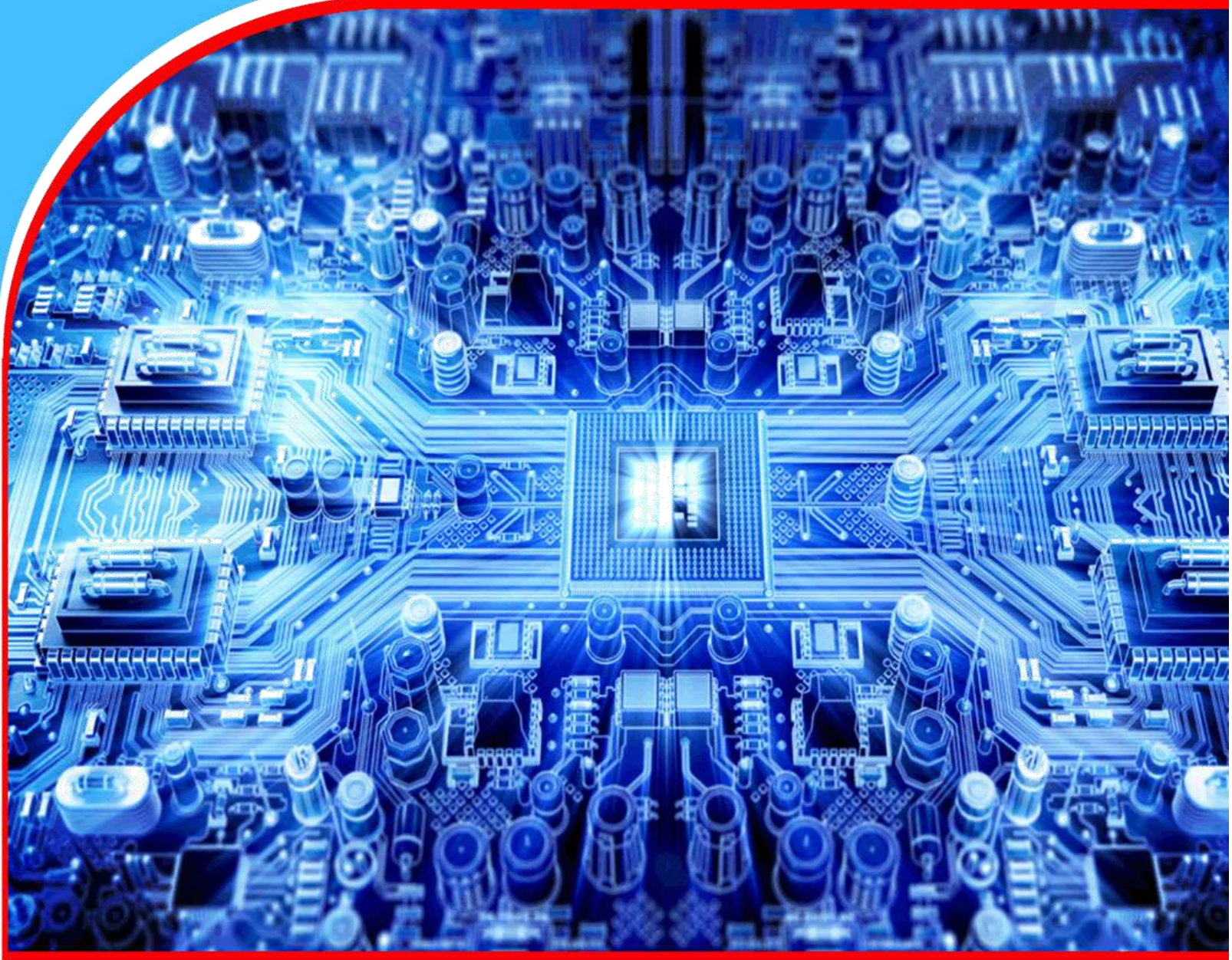

Diagnosis of Diabetic Retinopathy Utilizing Computer-Aided Diagnosis System

Hattan Omar Mujalled

Prof. Yasser Kadah

American Journal of Computing and Engineering
ISSN 2520-0449 (Online)
Vol.3, Issue 1, pp 1-23, 2020
www.ajpojournals.org

Diagnosis of Diabetic Retinopathy Utilizing Computer-Aided Diagnosis System

[1*]Hattan Omar Mujalled
Post Graduate Student: Faculty of Engineering
King Abdulaziz University
*Corresponding Author's E-mail: HMUJALLED0001@stu.kau.edu.sa

[2]Prof. Yasser Kadah
Lecturer, Faculty of Engineering
King Abdulaziz University

Abstract

Purpose: Diabetes is considered one of most diseases spread among people; blindness is considered the most resulted effect. Diabetes can damage the retinal blood vessels and cause severe problems to the eyes, which may end with sight loss. Such medical condition is known as "diabetic retinopathy" (DR). In such a diagnosis, the retinal microvascular go through several stages of change threat. In the early stages of the DR, detecting the formation that happened to the retinal blood vessels helps prevent the disease's dangerous effects. Therefore, producing a method to diagnose the disease in the early stages is helpful. So, this work aimed to develop a system of detecting and classifying the retina formation, trying to avoid relevant effects.

Methodology: The current method depends on vascular edges map extracted from images of retina captured by a fundus camera. Such a map been utilized to extract quantitative texture features. The system tested two independent groups of the region of interest in normal and abnormal images. The two sets were extracted from ground truth images of the 89 fundus images. Fundus images were annotated images from the Standard Diabetic Retinopathy Database (DIARETDB1).

Findings: The system provided an accuracy of 71% with a sensitivity of 75%.

Recommendation: The current work may open an opportunity for improvement for future work. Other methods may be reached to raise the accuracy and the sensitivity of the system. Besides, the current system may be tested on a larger sample size to study such effects. Finally, the ease of the current method makes it faster in adoption in the appropriate diagnosis especially in the early stages.

Keywords: *Computer-Aided Diagnosis; CAD; Diabetic Retinopathy; Fundus imaging; Image processing.*

1.0 INTRODUCTION

There are approximately 422 million adults who have diabetes around the globe. This figure has been multiplied around four times when backing to 1980. When considering the sinful daily lifestyle, life pressures, and challenging access to proper medications, such figures will continue rising [1]. By focusing on diabetes [2], there are several categories of disease linked: cardiovascular, neuropathy (nerve damage), Nephropathy (Kidney damage), Retinopathy (Eye damage), Foot damage, Skin conditions, Hearing impairment, Alzheimer's disease, and Depression.

In 2016, the world health organization (WHO) published a global diabetic report and considered the diabetic to be a significant cause of blindness [3]. Furthermore, in 2018 the same cause was the primary cause of vision loss. In this context, diabetes can damage the retinal blood vessels and cause severe problems to the eyes, which may end with sight loss. Also, many other vision conditions are the potential to have occurred, such as cataracts and glaucoma. This medical condition is known as "diabetic retinopathy" (DR). In such a diagnosis, the retinal microvascular goes through several changes that threaten the patient's vision. In different words, among the 20-60 years aged people worldwide, the most common diabetic complication is the DR, and it is the most common reason for blindness [4].

Regarding the DR prevalence, a study conducted in China shows that among 13473 diabetic participants, 34.08% suffers from DR. The study stated that patients' gender had no significant results [5]. Worldwide, the number of patients with DR is expected to rise from 126.6 million in 2010 to 191.0 million by 2030 [6]. A study conducted to measure the awareness level of diabetic patients about the DR, more than half of the tested sample (377 patients) did not think that their vision may be affected by DR. Furthermore, 35% never performed regular eye checkups [7]. In this context, the risk of becoming blind because of DR may dramatically be reduced to 50% by proper screening and diagnostics [8, 9]. Such screening action is recommended annually for the diabetic patient with no syndromes of either retinopathy or mild retinopathy by most of the guidelines [10].

1.1. Eye Anatomy and physiology

The human eye consists of several parts to complete the visual function. Figure 1.1 illustrates the major anatomical parts of the eye [11].

American Journal of Computing and Engineering
ISSN 2520-0449 (Online)
Vol.3, Issue 1, pp 1-23, 2020
www.ajpojournals.org

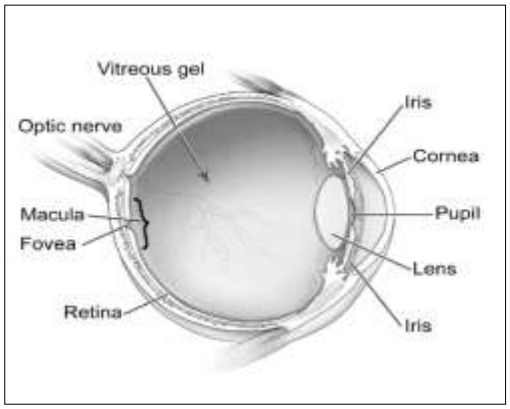

Figure 1.1: Anatomy of the eye

[11]

Undoubtedly, the retina is considered to be the most crucial part since it converts the light signals to electrical one so the brain can read signals through the optic nerve. Six classes of neurons perform the function of the retina. Five of them capture and process relevant signals, while one works as an organizational backbone [12]. Respectively, they are: Photoreceptors, bipolar cells, horizontal cells, amacrine cells, ganglion cells, and müllerianglia.

Parts of the retina starting from the internal limiting membrane back to the external limiting membrane can be shown in Fig. (1.2-1.3).

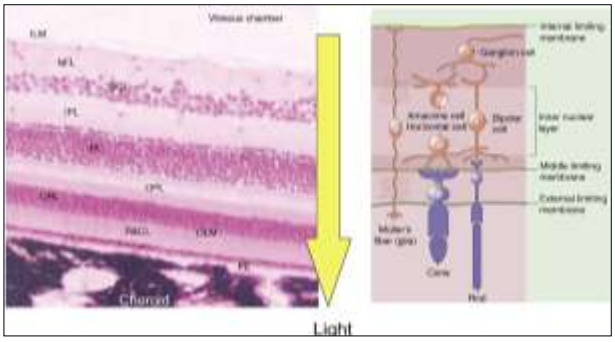

Figure 1.2: The cells and layers of the retina.

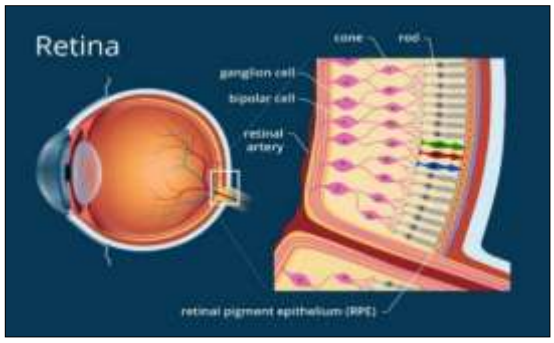

Figure 1.3: Retina structure [13]

[12]

1.2. Diabetic Retinopathy

According to the Harvard medical terms dictionary, diabetic retinopathy is defined as "a complication of diabetes that occurs when the small blood vessels in the retina are damaged. It can impair vision or even lead to blindness." [14]. Thus, the retinal blood vessel damage may start as abnormal swelling, or new retinal blood vessels may grow. As a result, the central vision area located in the macula affected by the retinal vessel leakage and the vision loss happened.

1.3. Clinical Types of Diabetic Retinopathy

Based on the blood vessels' condition in the retina and its induction of Proliferation, the DR is categorized into two classes: Non-proliferative DR, and Proliferative DR.

1.3.1. Non-Proliferative Diabetic Retinopathy (NPDR)

The changes in this level located within the retina and take several forms such as: micro-aneurysms, hemorrhages (small dot and blot splinter), intraretinal microvascular abnormalities (IRMA), and 'cotton wool' spots.

Concerning severity classes of the lesions, there are four classes of severity: mild, moderate, severe, and very severe.

1. Mild Non-Proliferative Diabetic Retinopathy

At this stage, all quadrants of the eye fundus have at least one lesion of microaneurysm and hemorrhages (dot, blot, or flame-shaped).

2. Moderate Non-Proliferative Diabetic Retinopathy

More severe microaneurysm and hemorrhages (dot and blot) appear in one to three quadrants. Also, at this stage, several indicators may appear, such as the cotton wool spots and changes in the level of venous caliber and beading. Also, mild microvascular abnormalities.

3. Severe Non-Proliferative Diabetic Retinopathy

One indicator of the following should be present at the minimum: All fundus quadrants include severe microaneurysms and hemorrhages, Two quadrants, as a minimum, include venous beading, and One quadrant, as a minimum, includes more severe microvascular abnormalities.

4. Very Severe Non-Proliferative Diabetic Retinopathy

To classify the NPDR as very sever, at least two of the three sever NPDR criteria need to be detected. Also, no indicators of proliferative DR should be present.

1.3.2. Proliferative Diabetic Retinopathy (PDR)

NPDR changes and lesions and microvascular capillary closures in retina result in tissue hypoxia. In such hypoxia cases, not enough oxygen is gained. As a result, new blood vessels are formed by vaso-proliferative factors to improve the oxygenation process to retina tissues. Neovascularization elsewhere (NVE) vessels are the name of newly formed vessels, and neovascularization of the disc (NVD) is the name of new vessels present on the optic disc. The next table summaries all four stages of NPDR and the PDR.

Table 1.1: Four stages of NPDR and the PDR.

Type of Diabetic Retinopathy	Stage	Location	Indicators
❖ Non-Proliferative Diabetic Retinopathy (NPDR)	1- Mild	All quadrants of the eye fundus.	• At least one lesion of microaneurysm and hemorrhages (dot, blot, or flame-shaped).
	2- Moderate	1 to 3 quadrants.	• More severe microaneurysm and hemorrhages (dot and blot). • Cotton wool spots, venous caliber changes including venous beading, and intraretinal microvascular abnormalities are present but mild.
	3- Severe	At least one case of the following three cases should appear:	
		All four quadrants of eye fundus.	• Severe hemorrhages and microaneurysms.
		At least two quadrants.	• Venous beading.
		At least one quadrant.	• More severe microvascular abnormalities.
	4- Very Severe	• at least 2 of the 3 sever NPDR criteria need to be detected. • No indicators of proliferative DR should be present.	
❖ Proliferative Diabetic Retinopathy (PDR)		• Retina (NVE). [1] • Optic disc (NVD).[2]	• Capillary closure. • New blood vessels are formed in order to improve the oxygenation process for retinal tissue.

[1] Neovascularization elsewhere (NVE) are new vessels growing on the retina.
[2] Neovascularisation of the disc (NVD) is new vessels growing on the optic disc.

The following images (Figure 1.4-1.7) are some examples of NPDR at different stages and PDR.

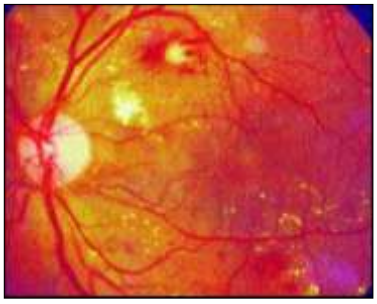

Figure 1.4: Moderate non-proliferative diabetic retinopathy

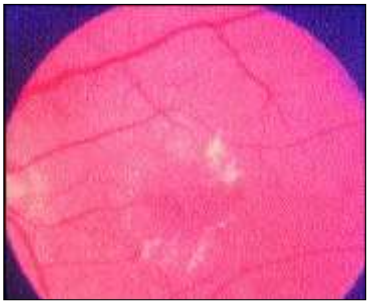

Figure 1.5: Diabetic maculopathy

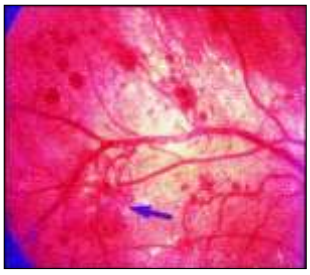

Figure 1.6: Proliferative diabetic retinopathy with neovascularization elsewhere..

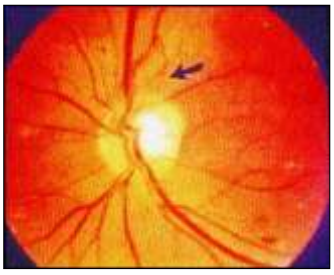

Figure 1.7: Proliferative diabetic retinopathy with neovascularization on the disc..

[4]

1.4. Research Motivation

DR is the most reason for blindness among diabetic patients. However, several health policies, especially of low- and medium-income countries, did not place DR on the top of their priories list. Also, there is a lack of awareness among patients about the severity of the danger staring them, besides difficulties of regular and routine diagnosing procedures concerning time, cost, and decision precision. These reasons triggered the work to investigate in design a computer-aided diagnosis (CAD) system that helped perform fast, precise diagnoses that assist the doctor and reduce false diagnoses based on human errors. Also, such a system will consider the high-cost issues and try to present a proper economic solution.

1.5. Objectives

This work proposes the following objectives:

- Find a reference database for funds images.
- Build a system with several stages to diagnose the presence of DR.

- Identify the level of severity of DR by such a system.

2.0 LITERATURE REVIEW

Distinct attributes can distinguish each stage of DR. Table 1.1 shows such attributes. All targeted indicators of DR appear in retinal images captured by a fundus camera. Retinal images are used for diagnosis since it holds a lot of information [15]. Undoubtedly, diseases had been detected in early stages possess higher opportunities to be treated [7-9, 15]. Therefore, the accurate and fast method needs to be designed to detect the DR in its current stage.

The aim of accuracy and fast diagnosis became possible with the assist of a computer algorithm to read the retinal images and classify them into the proper category. In the literature, several works touched the subject of diagnosing the DR from different points of view. A blood vessel segmentation algorithm was developed to eliminate improper patches [16]. Such segmentation was achieved by Bio-Geography Based Optimization utilizing the MATLAB optimization toolbox. The same issue of blood vessel segmentation was also studied in other research to separate the region of the optical disc from the retinal blood vessels [17]. On the other hand, some works focused on the DR classification. One of these research classifies the retinal images into one stage of different three stages of DR. It developed an algorithm that used Artificial Neural Network (ANN) classifiers [15].

In the same classification area, ANN was seen as a method with impacts concerning extended training time unless it was improved by hybridization with another algorithm [18]. Eye fundus from 1200 images was analyzed for DR detection. Concerning selected features, two types of extracted holistic texture and local retinal features were used. Neural networks, k-nearest neighbors, random decision forests, and support vector machines (SVM) classifiers were developed to reach work objectives. Best results were reached when SVM used to show an accuracy of 80.4% and a sensitivity of 82.2% [9].

Detection of mono conditions was conducted in some researches. For instance, Hard Exudates in retinal images were detected using a developed algorithm that used Random Forest (RF) and Back Propagation Neural Network (BPNN) classifiers. It shows the accuracy results of 92.12% with RF classifiers when using selected features [19]. In the same context, neovascularization[3] was detected using a methodology uses Gaussian filters, morphological features, and compactness classifier. The algorithm results were 89.4% for specificity and 63.9% for sensitivity [20]. Exudate detection was considered in several pieces of research. Mathematical morphological features were used to reach very high sensitivity and specificity of 80% and 99.5%, respectively [8].

3.0 RESEARCH METHODOLOGY

Research objectives achieved by developing an algorithm using MATLAB program[4] Following three main stages, the research's general methodology (Figure 3.1) was inspired by the previous

[3] *"New blood vessels grow due to extensive lack of oxygen in the retinal capillaries."*

[4] Program code available in the annex.

works [15, 21]. Three main stages are starting from selecting the proper databases to classify the severity of DR. Retinal images were extracted from open source databases such as DRIVE, MESSIDOR, and DIARETDB1 [22-24]. The following figure shows the general blocks of the research.

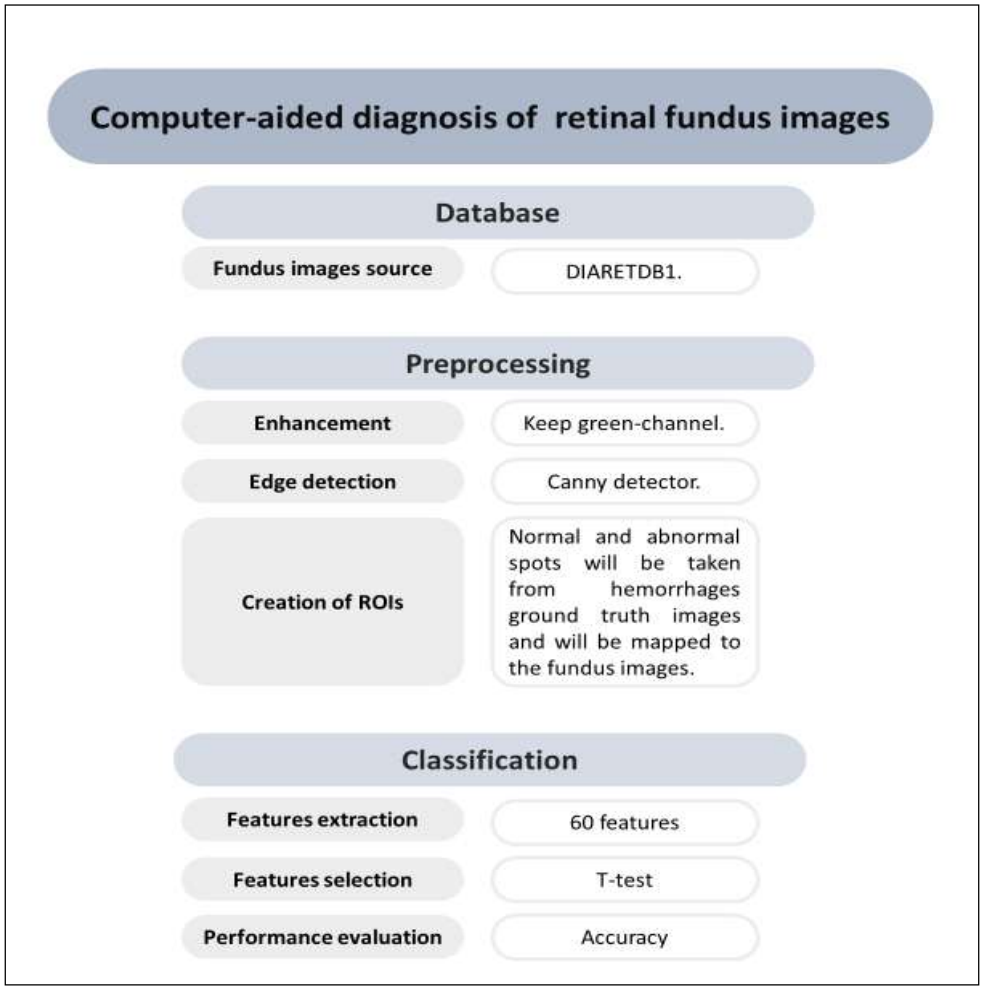

Figure 3.1: Methodology main stages

1.6. Database Creation

The research database was built from retinal images extracted from DIARETDB1 [22-24]. It is an open-source database available publicly for scientific research purposes. There are 89 colored funds retinal images[5] they were captured using the same 50-degree field-of-view digital fundus camera with varying imaging settings. The resolution of all images was the same (1500x1152).

[5] Images were taken in Kuopio university hospital in Finland.

There was no distinct population in terms of population distribution linked to selected images by medical experts.

The images are divided into 5 normal images free of DR signs, and 84 abnormal images show Microaneurysms signs. Ground truth images were structured by an image annotation software tool used by 4 medical experts. They have been asked independently to mark areas of interest to show lesions areas. Such areas included microaneurysms, hemorrhages, and hard and soft exudates. Figure 3.2 shows an example of the original retinal fundus image extracted from the DIARETDB1. Ground truth image example for each lesion found in one image can be illustrated in Figure 3.3.

Figure 3.2: Original retinal fundus image# 35.

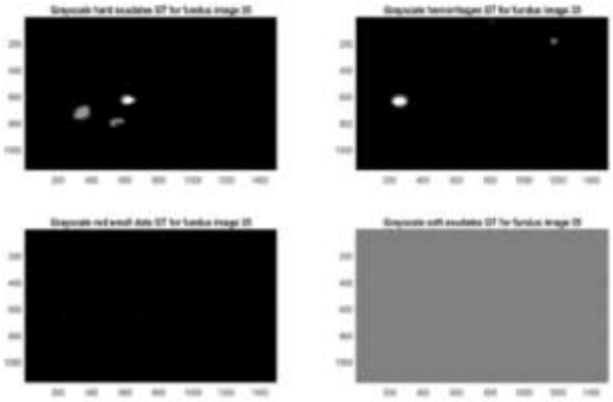

Figure 3.3: Ground truth for image# 35.

1.7. Preprocessing

A digital image is an array or matrix of square pixels arranged in rows and columns, and mathematically can be defined as a function of two variables [25]. Image processing considers operations performed on digital images to improve the image and utilize helpful information by segmenting the image's required parts. Image processing is also essential to eliminate the noise that may affect the quality of the image's information. Image processing operation varies to include enhancement and edge detection [25, 26].

Although the database images are colored, this work converted colored images into grayscale images using MATLAB tool to reduce the inherent complexity of colored images and ease image processing. The next figures (3.3-3.4) shows the grayscale image and colored one in once.

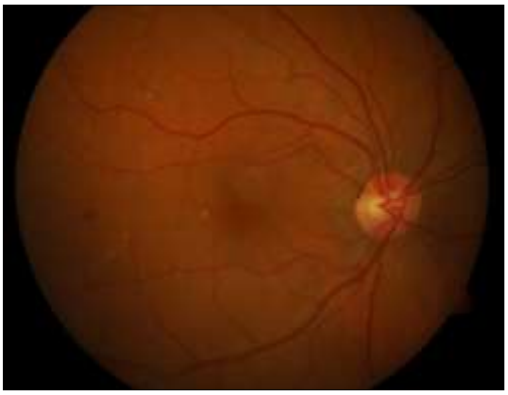

Figure 3.4: Colored fundus image# 35..

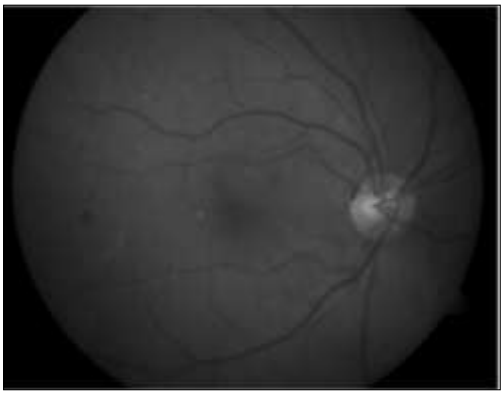

Figure 3.4: Colored fundus image# 35.

1.7.1. Image Enhancement

All alterations on digital images to make them easier to recognize key features are considered image enhancements operations. Enhancement techniques were used to sharpen images features to make them accepted visually and include more details.

1.7.1.1. Contrast Enhancement

Image Contrast shows how two or more parts of the image are different [27]. Thus, the greater the contrast, the easier to distinguish among different parts with the image. In this regard, since each image in the database is a combination of three layers matrix that form the RGB image. Each layer responsible for the representation of either red, green, or blue channels. The method of contrast encasement used is by isolating each channel and creating three single channels images for each image. By comparing the results, the channel that showed the most enhancement contrast was selected.

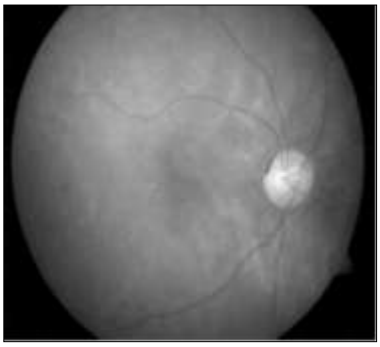

Figure 3.6: Red-channel image

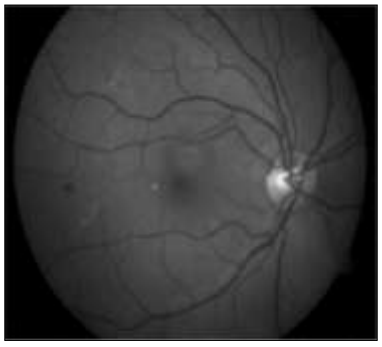

Figure 3.7: Green-channel image.

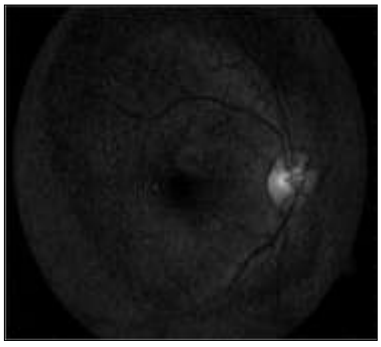

Figure 3.8: Blue-channel image.

As can be seen in the above three figures (3.5-3.7), the green channel gives the most significant differences among image objects and isolates them correctly from the background. Consequently, images with the green channel were selected in this research.

1.7.2. Removing Noise

The procedure of gathering data performed a source of noise for images captured from digital cameras [27]. Three different types of filters were applied to the green-channel images to reduce such noises in captured images. After that, the effects of filters were compared, and the best improvement in the images without changing in edges or objects details was assisted in selecting the filter.

1.7.2.1. Hampel Filter

Hampel filter is responsible for removing outliers in the image. It can be achieved by taking a window composed of median and another 6 samples, three on each side. The median absolute deviation estimates the standard deviation of each sample. The sample is replaced with the median if more than three standard deviations are different from the median.

Figure 3.9 shows the filtered image using the Hampel filter. Comparing to the non-filtered image, no clear different detected, and because of this, this filter was not selected.

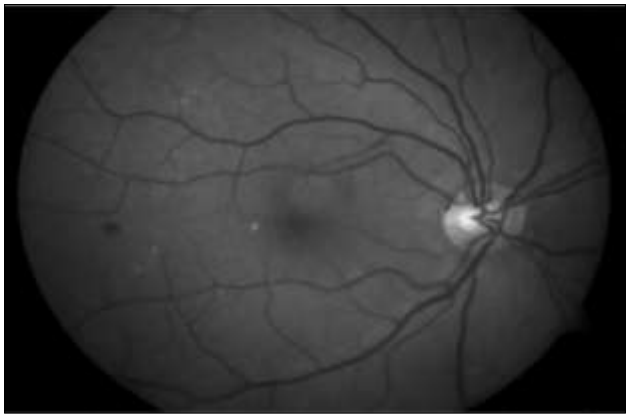

Figure 3.9: Hampel filter for green- channel image# 35.

1.7.2.2. Median Filter

The median filter is a nonlinear filter that works appropriately if edges are required to be kept. Each pixel represents the median of a 3-by-3 matrix neighborhood around the corresponding pixel from the input image in the output image. In terms of filtration results, images were smoother than the original ones. However, it was not selected since the difference was minimal comparing to the Wiener filter.

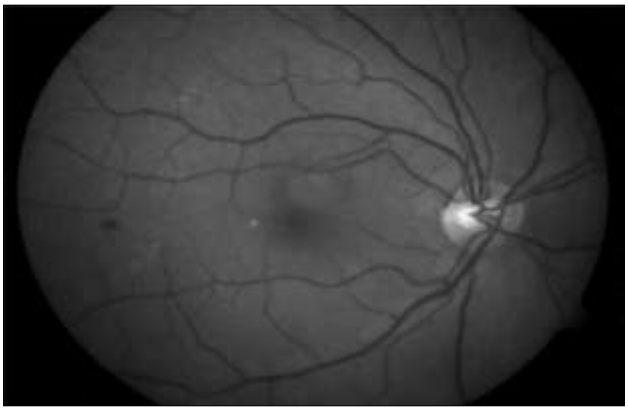

Figure 3.10: Median filter for green- channel image# 35.

1.7.2.3. Wiener Filter

As an adaptive filter, the Wiener filter adapts itself to the local image variance. The mean and the variance are calculated from the input image from the n-by-m matrix neighborhood around the corresponding pixel from the input image. Wiener filter performs little smoothing if the variance result is enormous. On the other hand, more smoothing is performed if the variance results are small.

Adaptive filters work correctly in case of high-frequency parts are exist, and edges are required to be preserved. It was because of the filters' selective performance rather than comparable performance, such as linear filters.

In this work, the n-by-m matrix neighborhood was selected to be [7 7] since the more significant matrices denoted images with little details. As shown in Figure 3.11, the Wiener filter results showed smoother areas with keeping all edges as in the original images.

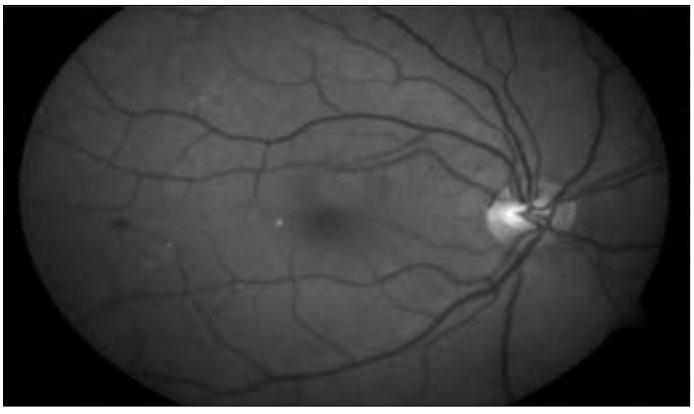

Figure 3.11: Wiener filter for green- channel image# 35.

Algorithms

The local mean and variance around each pixel are estimated by Wiener filter according to the following:

$$\mu = \frac{1}{NM} \sum_{n_1,n_2 \in \eta} a(n_1, n_2)$$

and

$$\sigma^2 = \frac{1}{NM} \sum_{n_1,n_2 \in \eta} a^2(n_1, n_2) - \mu^2$$

where η is the N-by-M local neighborhood of each pixel in image A.

wiener filter then creates a pixel-wise using these estimates,

$$b(n_1, n_2) = \mu + \frac{\sigma^2 - v^2}{\sigma^2}(a(n_1, n_2) - \mu)$$

where v^2 is the noise variance. If the noise variance is not given, wiener uses the average of all the local estimated variances.

1.7.3. Edge Detection

The boundaries among objects, overlapped objects, and the same image's background are distinguished by edges[28]. In disease detection and classification, edge detection plays an essential rule in image processing to increase results[29]. Brightness discontinues in the images generate edges. There are several algorithms in MATLAB to detect them known as detectors. Standard edge detectors used are Sobel, Canny, Prewitt, Roberts. In this regard, the edge detector that shows more boundaries was considered the selected one, and then it was used on the filtered image.

1.7.3.1. Sobel Detector

Sobel detector is considered a derivative operator that includes two matrices working on the image to distinguish edges of the image. These two matrices, known as masks, are responsible for prominent vertical and horizontal edges of the image. For image H, the Sobel detector S, the vertical mask S_x and the horizontal mask S_y work as the following:

$$S_x = \begin{pmatrix} -1 & 0 & 1 \\ -2 & 0 & 2 \\ -2 & 0 & 1 \end{pmatrix} * H \text{ and } S_y = \begin{pmatrix} -1 & -2 & -1 \\ 0 & 0 & 0 \\ 1 & 2 & 1 \end{pmatrix} * H$$

So, the convolution of the image with the vertical mask was prominent in the vertical edges. The convolution with the horizontal mask will be prominent in the horizontal edges of the image.

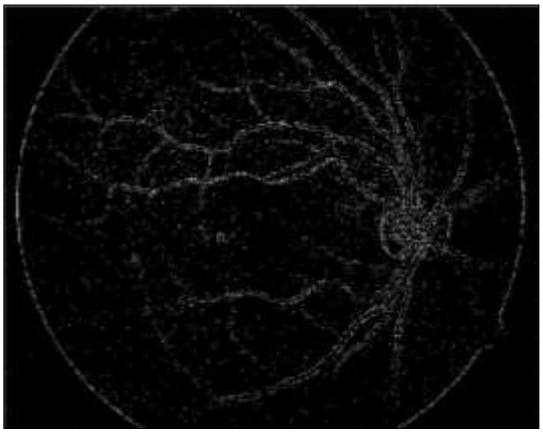

Figure 3.12: Sobel edge detector

As can be noticed from Figure 3.12, the image after the Sobel detector still has areas with unclear edges. Based on this, it will not be selected.

1.7.3.2. Canny Detector

Most literature reported that Canny detectors are the most suitable ones due to less false edges; it gives [30, 31]. It is a multistage algorithm known widely as the standard edge detector in several perspectives of image processing to distinguish sharp intensity variations. The multistage of the Canny detector can be summarized as the following: Removing noise by applying Gaussian filter, Searching image intensity gradients, Applying non-maximum suppression to remove artificial response to edge detection, and Locating potential edges by applying a double threshold, Tracking all other edges and eliminate those who are weak and not connected to high intense edges.

In other words, the edges in the Canny detector are performed by applying the Gaussian filter on the input image to reduce the noise. After that, the gradient magnitude and direction on each pixel are determined. Then at each pixel, if the gradient magnitude was larger than the gradients of the two neighbors in the gradient direction, the pixel was marked as an edge. Otherwise, the pixel was marked as background. Finally, the weak edges were removed by the hysteresis thresholding.

The next Figure 3.13 shows the effect of Canny detectors on the images of this research. The edges were precise, and many details been shown. Thus, the Canny detector was selected.

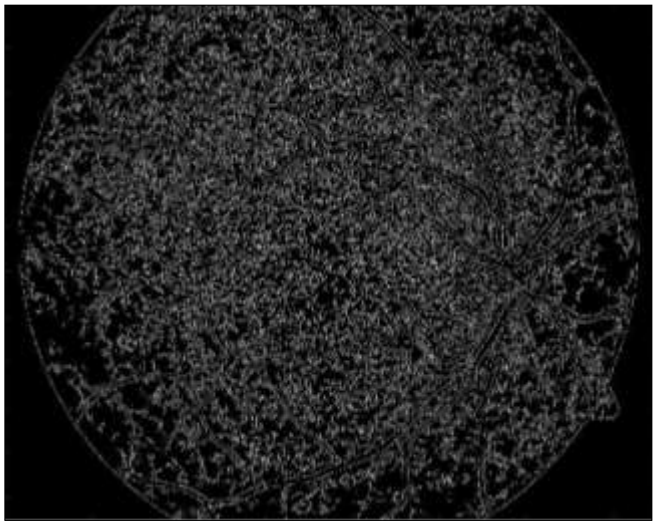

Figure 3.13: Canny edge detector without filtering.

After selecting the Canny detector, it was applied to filtered images, and the result can be seen in Figure 3.14.

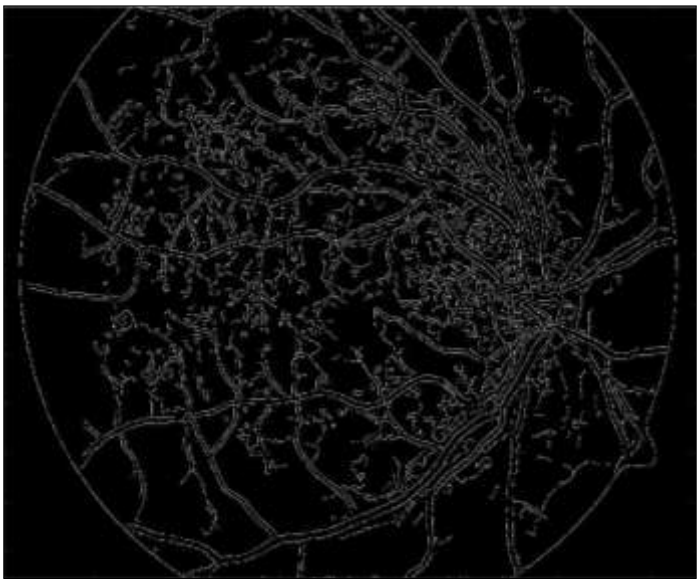

Figure 3.14: Canny edge detector for wiener filtered green-channel image# 35

1.7.3.3. Prewitt Detector

Prewitt detector is a derivative operator, and the same principle applied in the Sopel detector is applied in the Prewitt operator. The difference is in the direction of the gradient. Comparing output images from Prewitt detectors to Sopel detectors results, images were very similar, and more edges disappeared.

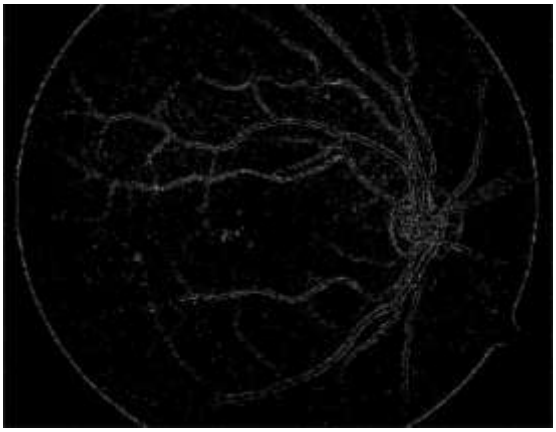

Figure 3.15: Prewitt edge detector.

1.7.3.4. Roberts Detector

When comparing images after applying Sobel and Prewitt detectors to images using Roberts detectors, the results are images with more noise and unclear edges. Undoubtedly, the Robert operator will not be preferred.

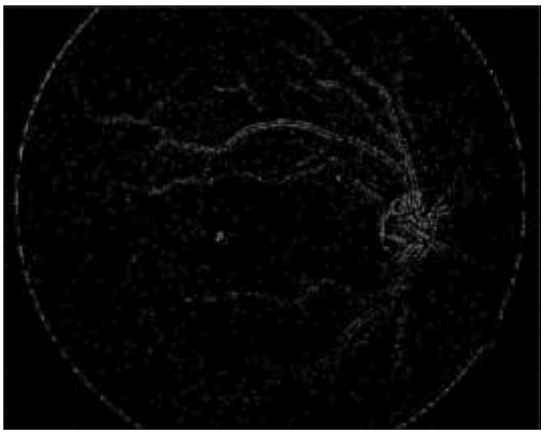

Figure 3.16: Robert edge detector.

1.8. Creation of Region of Interest

The ground truth images of hemorrhages were considered the system's reference to creating the two groups of the normal and abnormal region of interests (ROI). Total ROIs were decided to reach 840. This total ROIs were divided equally into 420 abnormal and normal locations were

extracted from the ground truth images. Then, all locations were mapped into processed fundus images.

1.9. Features Extraction

There are 60 features extracted to perform the classification process. These features shown in table 3.1 were divides into 5 main parts according to the type of processing. They are:

- Basic
- Differences (diff)
- 2-D fast Fourier transform (fft2)
- Histogram (hist)
- Gray-level co-occurrence matrix (GLCM)

Table 3.1: List of extracted features.

Feature group	Feature	Feature group	Feature
Feature 1	mean	**Feature 31**	sum of histogram multiplied by log
Feature 2	standard deviation	**Feature 32**	squeeze
Feature 3	maximum	**Feature 33**	squeeze multiplied by log
Feature 4-8	percentiles of a data set	**Feature 34**	mean of GLCM
Feature 9	mean diff	**Feature 35-39**	percentiles of a GLCM data set
Feature 10	standard deviation diff	**Feature 40**	GLCM mean diff
Feature 11	maximum diff	**Feature 41**	GLCM std diff
Feature 12-27	FFT2	**Feature 42**	GLCM maximum diff
Feature 28	standard deviation of FFT2	**Feature 43-58**	GLCM FFT2
Feature 29	Maximum of FFT2	**Feature 59**	GLCM standard deviation of FFT2
Feature 30	sum of histogram	**Feature 60**	GLCM maximum of FFT2

1.10. Features Selection

The t-test was utilized to filter the features rand selecting the useful ones to utilize the inferential statistical tools. The P-value was selected to be 5%. The result of the t-test reduced the features from 60 to 27 useful features. The list of selected features is shown in table 3.2.

Table 3.2: List of selected features.

Feature group	Feature	Feature group	Feature
Feature 1	mean	**Feature 33**	squeeze multiplied by log
Feature 2	standard deviation	**Feature 43**	GLCM FFT2
Feature 9	mean diff	**Feature 45**	
Feature 10	standard deviation diff	**Feature 46**	
Feature 17	FFT2	**Feature 47**	
Feature 18		**Feature 48**	
Feature 19		**Feature 52**	
Feature 21		**Feature 53**	
Feature 24		**Feature 54**	
Feature 26		**Feature 56**	
Feature 27		**Feature 57**	
Feature 30	sum of histogram	**Feature 59**	GLCM standard deviation of FFT2
Feature 31	sum of histogram multiplied by log	**Feature 60**	GLCM maximum of FFT2
Feature 32	squeeze	---	---

4.0 PRESENTATION OF FINDINGS, ANALYSIS AND INTERPRETATION

Two types of results were conducted to judge the system. The general results that give a general indication of how the system works. However, many factors play important roles when deciding the appropriate classifiers. So, the contingency matrix elements results were considered as the second type of result.

4.1. Classification

After running the system, several results were shown among the tested classifiers. The first indication of classification was the error rate for each one. The next Figure 4.1 shows all error rates of classifiers. This level of examination is considered as primary assessment. However, there is a need to examine other factors to reach a rationale for selecting an appropriate classifier.

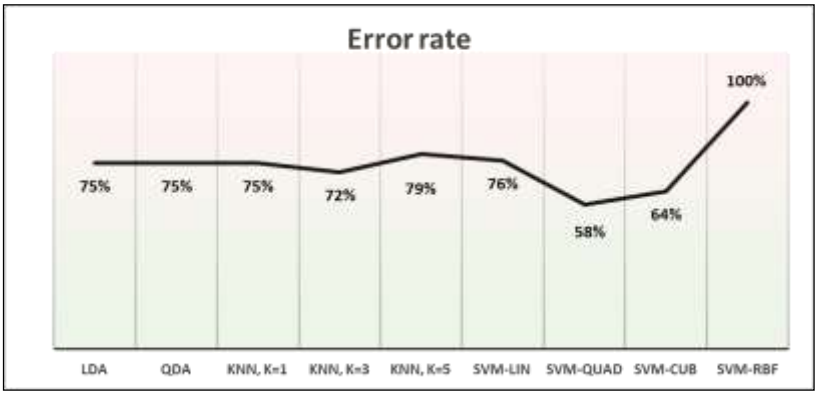

Figure 4.1: Classifiers' error rates.

Refereeing to Figure 4.1, most classifiers' error rates were placed in the range of 72% - 79%. There was only one classifier that showed a full error rate of 100%. On the other hand, SVM-QUAD and SVM-CUB were assessed as classifiers with the least error rates of 58% and 64%, respectively.

4.2. Performance Evaluation

Assessing the results of different classifiers was through the Contingency matrix. In this matrix, the performance of each classifier was evaluated in terms of:

- **Accuracy**: which reflects the global reliability.
  - $ACC = \frac{TP+TN}{TP+TN+FP+FN}$ (4.1)
- **Sensitivity**: which represents the ability of identifying the presence of the disease.
  - $Sens = \frac{TP}{(TP+FN)}$ (4.2)
- **Specificity**: which represents the ability of identifying the absence of the disease.
  - $Spec = \frac{TN}{TN+FP}$ (4.3)
- **Positive predictive value** (PPV): represent the reliability of the positive results.
  - $PPV = \frac{TP}{TP+FP}$ (4.4)
- **Negative predictive value** (NPV): which reflect how we can rely on the classifier in identifying of negative results.
  - $NPV = \frac{TN}{TN+FN}$ (4.5)

All measures mentioned above are based on 4 main variables in terms of either the positive or negative result was diagnosed truly or not. The 4 main variables are:

- **True positives (TP)**: which reflects the positive results diagnosed truly.
- **False positive (FP)**: which reflects the positive results not diagnosed truly.
- **True negative (TN)**: which reflects the negative results diagnosed truly.
- **False negative (FN)**: which reflects the negative results not diagnosed truly.

The next Figure 4.2 show the relation among the variables of the Contingency matrix.

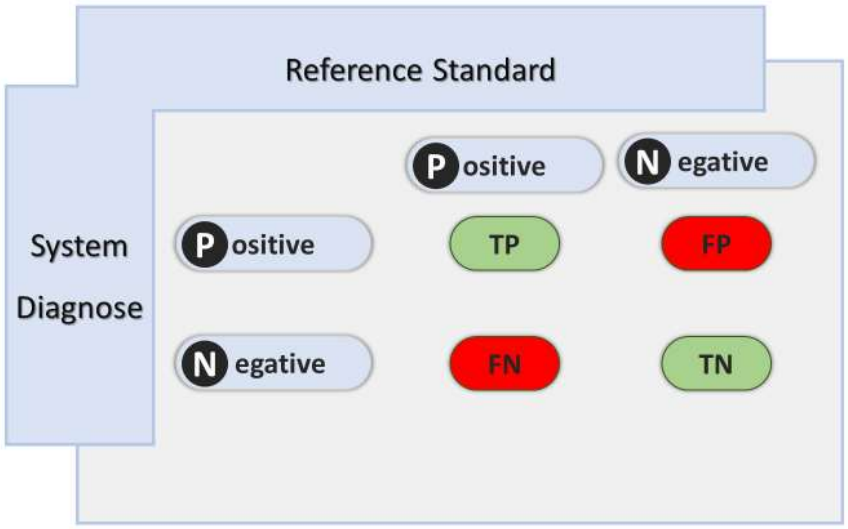

Figure 4.2: Contingency matrix.

All results were extracted as can be shown in the following table 4.1.

Table 4.1: Classifiers complete performance evaluation.

	LDA	QDA	KNN, K=1	KNN, K=3	KNN, K=5	SVM-Lin	SVM-Quad	SVM-Cub
Acc	62%	62%	62%	64%	60%	62%	**71%**	68%
Sens	67%	67%	67%	70%	67%	60%	**75%**	81%
Spec	60%	60%	60%	61%	58%	64%	**68%**	63%
PPV	49%	49%	49%	49%	42%	70%	**62%**	47%
NPV	75%	75%	75%	79%	79%	54%	**79%**	89%

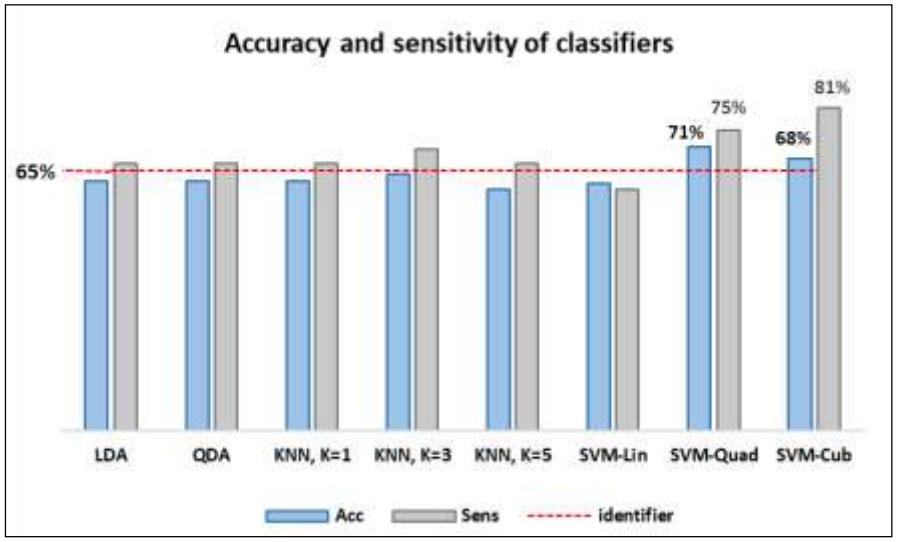

Figure 4.3: Performance evaluation of classifiers.

The seventh classifier, the SVM-Quad, shows the highest accuracy of 71% over other classifiers. Also, the sensitivity results were acceptable compared to the most sensitive classifier, the SVM-Cub. Both classifiers had acceptable results in terms of sensitivity, and results were close to each other. Although the SVM-Cub shows the highest NPV value, the SVM-Quad result for the same figure of NPV was 79%, which is considered acceptable and close to the 89% one of SVM-Cub. SVM-Quad's PPV reading was around 5% better than the PPV for the SVM-Cub with 62%. The SVM-Quad was selected as the best choice since the reliability of identifying the positive and negative cases of PPV and NPV was balanced and close to each other.

5.0 SUMMARY, CONCLUSIONS AND RECOMMENDATION

Early detection for diseases can help in vital prevention, especially for diabetic patients. One condition that is considered as a primary reason for blindness is diabetic retinopathy (DR). Detecting the DR in the early stages may help in reducing the number of patients lose their sight. In this work, the CAD system was created to help in classifying the patient disease stage. The system tested two independent groups of the region of interest in normal and abnormal images. The two sets were extracted from ground truth images of the 89 fundus images. Fundus images were annotated images from the Standard Diabetic Retinopathy Database (DIARETDB1). The system provided an accuracy of 71% with a sensitivity of 75%. The current work may open an opportunity for improvement for future work. Other methods may be reached to raise the accuracy and the sensitivity of the system. Besides, the current system may be tested on a larger sample size to study such effects. Finally, the ease of the current method makes it faster in adoption in the appropriate diagnosis especially in the early stages.

References

[1] WHO, "Diabetes: key facts," vol. 2018, ed: world health organisation, 2018.
[2] MAYO-CLINIC. "Diabetes." Mayo Foundation for Medical Education and Research (MFMER). https://www.mayoclinic.org/diseases-conditions/diabetes/symptoms-causes/syc-20371444?p=1 (accessed 10-Nov-2018, 2018).
[3] WHO, "Global report on diabetes," World Health Organization; 1 edition (May 31, 2016), world health organisation, 9789241565257, 2016. [Online]. Available: http://www.who.int/iris/handle/10665/204871
[4] K. Viswanath and D. D. M. McGavin, "Diabetic retinopathy: clinical findings and management," *Community eye health*, vol. 16, no. 46, pp. 21-24, 2003.
[5] Y. Liu *et al.*, "Prevalence of diabetic retinopathy among 13473 patients with diabetes mellitus in China: a cross-sectional epidemiological survey in six provinces," *BMJ Open*, 10.1136/bmjopen-2016-013199 vol. 7, no. 1, 2017.
[6] Y. Zheng, M. He, and N. Congdon, "The worldwide epidemic of diabetic retinopathy," *Indian journal of ophthalmology*, vol. 60, no. 5, pp. 428-431, Sep-Oct 2012, doi: 10.4103/0301-4738.100542.
[7] S. H. Alzahrani *et al.*, "Awareness of diabetic retinopathy among people with diabetes in Jeddah, Saudi Arabia," *Therapeutic advances in endocrinology and metabolism*, vol. 9, no. 4, pp. 103-112, 2018, doi: 10.1177/2042018818758621.
[8] A. Sopharak, B. Uyyanonvara, S. Barman, and T. H. Williamson, "Automatic detection of diabetic retinopathy exudates from non-dilated retinal images using mathematical morphology methods," *Computerized Medical Imaging and Graphics*, vol. 32, no. 8, pp. 720-727, 2008/12/01/ 2008, doi: https://doi.org/10.1016/j.compmedimag.2008.08.009.
[9] L. B. Frazao, N. Theera-Umpon, and S. Auephanwiriyakul, "Diagnosis of diabetic retinopathy based on holistic texture and local retinal features," *Information Sciences*, vol. 475, pp. 44-66, 2019/02/01/ 2019, doi: https://doi.org/10.1016/j.ins.2018.09.064.
[10] V. Gulshan, L. Peng, M. Coram, and et al., "Development and validation of a deep learning algorithm for detection of diabetic retinopathy in retinal fundus photographs," *JAMA*, vol. 316, no. 22, pp. 2402-2410, 2016, doi: 10.1001/jama.2016.17216.
[11] NEI. "NEI photos and images." National Eye Institute (NEI). https://nei.nih.gov/photo (accessed 16-11-2018, 2018).
[12] C. E. Willoughby, D. Ponzin, S. Ferrari, A. Lobo, K. Landau, and Y. Omidi, "Anatomy and physiology of the human eye: effects of mucopolysaccharidoses disease on structure and function – a review," *Clinical & Experimental Ophthalmology*, vol. 38, no. s1, pp. 2-11, 2010, doi: 10.1111/j.1442-9071.2010.02363.x.
[13] O. Gary Heiting. "The Retina: Where Vision Begins." AAV Media, LLC. © 2000-2018 AAV Media, LLC. https://www.allaboutvision.com/resources/retina.htm (accessed 16-11-2018.
[14] Harvard, "definition of diabetic retinopathy," in *Medical Dictionary of Health Terms*, H. M. School, Ed., ed, 2011.
[15] B. G. Khandare S, Gaffar S, Upadhyay A,, "AUTOMATIC DETECTION OF BLOOD VESSELS AND CLASSIFICATION OF RETINAL IMAGE INTO DIFFERENT STAGES OF DIABETIC RETINOPATHY," 2018, 2395-0056. [Online]. Available: https://www.irjet.net/volume5-issue4.
[16] R. Adalarasan and R. Malathi, "Automatic Detection of Blood Vessels in Digital Retinal Images using Soft Computing Technique," *Materials Today: Proceedings*, vol. 5, no. 1, Part 1, pp. 1950-1959, 2018/01/01/ 2018, doi: https://doi.org/10.1016/j.matpr.2017.11.298.

[17] D. S. S. Raja and S. Vasuki, "Automatic detection of blood vessels in retinal images for diabetic retinopathy diagnosis," *Computational and mathematical methods in medicine*, vol. 2015, pp. 419279-419279, 2015, doi: 10.1155/2015/419279.
[18] R. Bala and D. D. Kumar, "Classification Using ANN : A Review," 2017.
[19] K. Akyol, a. Bayir, B. En, and H. B. Akmak, "Detection of Hard Exudates in Retinal Fundus Images based on Important Features Obtained from Local Image Descriptors," *Journal of Computer Sciences and Applications*, vol. 4, no. 3, pp. 59-66, 2016/11/29 2016, doi: 10.12691/jcsa-4-3-2.
[20] S. S. A. Hassan, D. B. L. Bong, and M. Premsenthil, "Detection of neovascularization in diabetic retinopathy," *Journal of digital imaging*, vol. 25, no. 3, pp. 437-444, 2012, doi: 10.1007/s10278-011-9418-6.
[21] Z. Abduh, M. A. Wahed, and Y. M. Kadah, "Robust Computer-Aided Detection of Pulmonary Nodules from Chest Computed Tomography," *Journal of Medical Imaging and Health Informatics*, vol. 6, no. 3, pp. 693-699, // 2016, doi: 10.1166/jmihi.2016.1731.
[22] J. Staal, M. D. Abramoff, M. Niemeijer, M. A. Viergever, and B. v. Ginneken, "Ridge-based vessel segmentation in color images of the retina," *IEEE Transactions on Medical Imaging*, vol. 23, no. 4, pp. 501-509, 2004, doi: 10.1109/TMI.2004.825627.
[23] MESSIDOR. Methods to evaluate segmentation and indexing techniques in the field of retinal ophthalmology. [Online] Available: http://www.adcis.net/en/Download-Third-Party/Messidor.html
[24] T. Kauppi *et al.*, *DIARETDB1 diabetic retinopathy database and evaluation protocol*. 2007.
[25] B. B, *A STUDY ON THE IMPORTANCE OF IMAGE PROCESSING AND ITS APLLICATIONS*. 2014, pp. 155-160.
[26] P. M. Ingale, "*The importance of Digital Image Processing and its applications*," *International Journal of Scientific Research in Computer Science and Engineering*, vol. 06, no. 01, pp. 31-32, 2018.
[27] N. Ahmed and W. Ahmed, *The Application of Image Enhancement on Color and Grayscale Images*. 2019.
[28] S. Saini, B. Kasliwal, and S. Bhatia, "Comparative Study Of Image Edge Detection Algorithms," *CoRR*, vol. abs/1311.4963, / 2013.
[29] G. Yang and F. Xu, "Research and analysis of Image edge detection algorithm Based on the MATLAB," *Procedia Engineering*, vol. 15, pp. 1313-1318, 2011/01/01/ 2011, doi: https://doi.org/10.1016/j.proeng.2011.08.243.
[30] S. Katiyar and A. P V, *Comparative analysis of common edge detection techniques in context of object extraction*. 2012, pp. 68-78.
[31] L. Ding and A. Goshtasby, "On the Canny edge detector," *Pattern Recognition*, vol. 34, no. 3, pp. 721-725, 2001/03/01/ 2001, doi: https://doi.org/10.1016/S0031-3203(00)00023-6.